Chemistry & Biology 13, 531–538, May 2006 DOI 10.1016/j.chembiol.2006.03.009

Mimicking Helical Antibacterial Peptides with Nonpeptidic Folding Oligomers

Aude Violette,[1] Sylvie Fournel,[1] Karen Lamour,[1] Olivier Chaloin,[1] Benoit Frisch,[2] Jean-Paul Briand,[1] Henri Monteil,[3] and Gilles Guichard[1,*]

[1] Immunologie et Chimie Thérapeutiques
UPR 9021 CNRS
Institut de Biologie Moléculaire et Cellulaire
15 rue René Descartes
F-67084 Strasbourg Cedex
France

[2] Laboratoire de Chimie Bioorganique
UMR 7514 CNRS-ULP
Faculté de Pharmacie
74 route du Rhin
F-67400 Illkirch
France

[3] Laboratoire de Physiopathologie et d'Antibiologie des Infections Nosocomiales et Emergentes
Institut de Bactériologie
Faculté de Médecine
3 rue Koeberlé
F-67000 Strasbourg
France

Summary

Unnatural oligomeric scaffolds designed to adopt defined secondary structures (e.g., helices), while retaining the chemical diversity of amino acid side chains, are of practical value to elaborate functional mimetics of bioactive α-polypeptides. Enantiopure *N,N′*-linked oligoureas as short as seven residues long have been previously shown to fold into a stable helical structure, stabilized by 12- and 14-membered H-bonded rings. We now report that eight-residue oligoureas designed to mimic globally amphiphilic α-helical host-defense peptides are effective against both gram-negative and gram-positive bacteria (including methicillin-resistant *Staphylococcus aureus* [MRSA]) and exhibit selectivity for bacterial versus mammalian cells. Circular dichroism (CD) spectroscopy studies suggest enhanced helical propensity of oligoureas in the presence of phospholipid vesicles. The utility of this new class of nonpeptidic foldamers for biological applications is highlighted by high resistance to proteolytic degradation.

Introduction

Antimicrobial α-peptides that adopt cationic amphipatic structures (e.g., α helices) upon binding to cell membranes (e.g., melittin from bee venom [1], magainins from frog skin [2], cecropins from porcine small intestine [3]) are ubiquitous in nature and represent important effector molecules of innate immunity [4]. They exhibit narrow to broad spectrum of activity against gram-positive and/or gram-negative bacteria. Most importantly, synthetic cationic peptides compared to conventional antibiotics possess a low potential for the induction of bacterial resistance [5, 6], which makes them attractive candidates for the development of therapeutically useful antimicrobial agents [4, 7].

Cationic antimicrobial peptides are believed to cause cell death by a two-step mechanism involving interaction with the lipid component of the membrane and membrane permeabilization [8]. Several mechanisms for membrane permeabilization have been postulated including transient pore formation ("barrel-stave model") or detergent-like disruption of the membrane ("carpet model"). The outer leaflet of the bacterial membrane is essentially composed of lipids with negatively charged phospholipid headgroups, whereas in plants and animals, it is almost zwitterionic and rich in cholesterol. As a result, some cationic host-defense peptides, within certain concentration limits, exhibit selectivity for bacterial membranes versus human cells because of preferential electrostatic interactions. The lytic activity and membrane selectivity of amphiphilic antimicrobial peptides are strikingly dependent on properties such as helix stability, amphiphilicity (hydrophobic moment), hydrophobicity, relative width of the hydrophilic and hydrophobic faces of the helix, as well as net charge. Structure activity relationship studies remain challenging because sequence modifications of α-peptides generally affect several parameters at the same time [9, 10].

Alternatively, the finding that unnatural oligoamide backbones can adopt well-defined and controlled helical secondary structures suggested that one could use them as scaffolds to distribute charged side chains in a predictable manner for de novo design of cationic amphiphilic molecules mimicking natural host defense α-peptides (for reviews see [11–13]). Antimicrobials based on either β-peptides 3_{14}, 2.5_{12}, and $2.7_{10,12}$ helical folds [14–18] or on peptoids polyproline type I-like helix [19] have been described. Yet, antimicrobial properties of helix-forming peptidomimetics other than oligoamides have not been documented.

N,N′-linked oligoureas **A** (also denoted PG-[β-HXaa^{u}]$_n$-NH$_2$) with proteinogenic side chains are peptide backbone mimetics that belong to the γ-peptide lineage. They are formally obtained by simple substitution of NH for the $^{\alpha}CH_2$ of the amino acid constituents of γ^4-peptides. We have shown recently, by using combination of NMR spectroscopy and circular dichroism, that oligoureas as short as seven residues can adopt a stable right-handed *2.5*-helical secondary structure stabilized by 12- and 14-membered H-bonded rings (Figure 1A) in various solvents such as pyridine, methanol, and trifluoromethanol [20–22] reminiscent of the helix described for the corresponding γ^4-peptides. This strong helix folding propensity, together with the diversity of available side chain appendages and the expected resistance to protease degradation, make the oligourea backbone a promising candidate for biomedical applications.

Herein, we report on the de novo design and synthesis of short-chain amphiphilic cationic oligoureas **1–13** (Figure 1B) and evaluation of their antimicrobial properties.

*Correspondence: g.guichard@ibmc.u-strasbg.fr

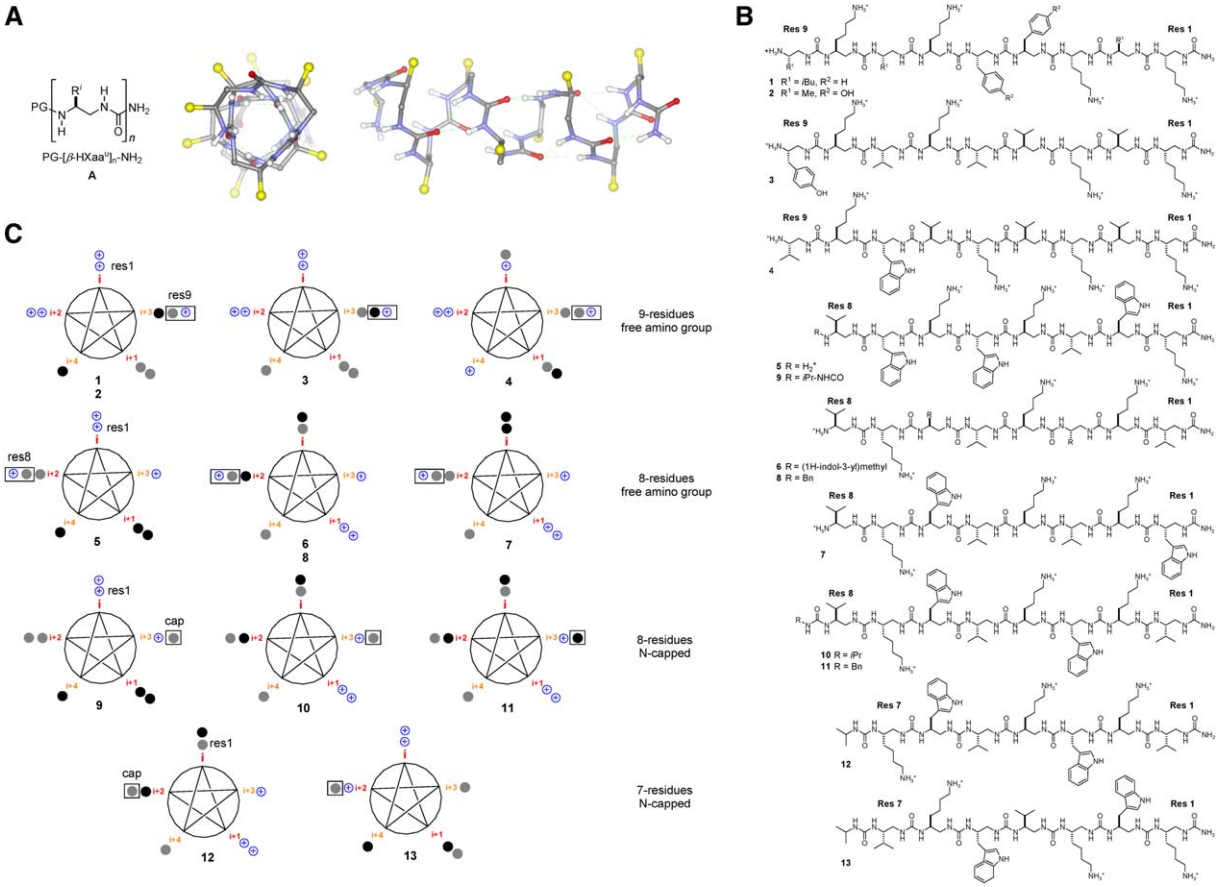

Figure 1. Design of Amphipathic Cationic *N,N′*-Linked Oligoureas

(A) General formula of *N,N′*-linked oligoureas and schematic representation of the idealized (*P*)-$2.5_{12,14}$ helix (side view and top view) highlighting the five residue repeat.

(B and C) Sequences and helical wheel representation of amphiphilic *2.5*-helical oligoureas evaluated for antimicrobial activity. These oligoureas are exclusively composed of cationic side chains (β-HLys^u, indicated by a plus sign) segregated on two-fifth (1–3, 5–13) or three-fifth (4) of the helix circumference and hydrophobic aliphatic (indicated by a closed circle) and aromatic (indicated by a closed circle) side chains. A terminal residue with a free amino group on the west side of the molecule is indicated by a plus sign and a closed circle or a plus sign and a closed circle in a box, while an *N*-capped terminus is indicated by a closed circle or a closed circle in a box.

Results and Discussion

Amphiphilic oligoureas **1–13**, ranging from seven to nine residue long were designed assuming an idealized *2.5*-helical structure as illustrated on Figure 1C. Cationic hydrophilic residues with side chain of lysine (β-HLys^u) were arranged to create a polar surface that roughly covers two-fifth (**1–3** and **5–13**) or three-fifth (**4**) of the helix circumference (Figure 1C). The remaining hydrophobic face was formed from a selection of residues with aliphatic (Me, *i*Pr, and *i*Bu) and aromatic (Bn, 4-HO-$C_6H_4CH_2$,(1*H*-indol-3-yl)methyl) side chains. Oligoureas **1–13** were synthesized on Rink amide resin with *N*-Fmoc protected building blocks as previously described [19, 23] and were purified to >95% homogeneity by C_{18} RP-HPLC. Although Fmoc/tBu chemistry on solid support is convenient and was previously found to be suitable for the synthesis of oligoureas with Ala, Val, Phe, Tyr, and Lys side chains up to nonamers [20–23], it showed some limitations in the course of the synthesis of a number of oligoureas reported here, which were recovered in low yields after HPLC purifications. Recent investigations with N-Boc protected monomers [24] have shown that Boc chemistry represents a useful alternative to the preparation in high yields of amphiphilic oligourea sequences incorporating functionalized side chains (A.V., unpublished data).

In primary screening experiments (Table 1), antibacterial activity was assayed against a representative set of gram-positive (*Staphylococcus aureus* [*S. aureus*] American-type culture collection [ATCC] 25923) and gram-negative (*Escherichia coli* [*E. coli*] ATCC 25922, *Pseudomonas aeruginosa* [*P. aeruginosa*] ATCC 27853) bacteria cultured in brain-heart broth. Minimal inhibitory concentration (MIC) as well as minimal bactericidal concentration (MBC) were determined after a 20 hr incubation at 35ºC in air. The α-helical α-peptide melittin from bee venom [1] served as a positive control.

The first molecules examined in this study, namely nonamers **1–4**, had a comparable net charge but differed in the composition of hydrophobic residues (β-HLeu^u, β-HPhe^u **[1]**; β-HAla^u, β-HTyr^u **[2]**; β-HVal^u, β-HTyr^u **[3]**; β-HVal^u, β-HTrp^u **[4]**). Surprisingly, despite propensity for helix formation in MeOH (monitored by CD at 203 nm) (Figure 2A) [22] and amphiphilic character, none of these molecules did show significant antibacterial activity

Table 1. Antimicrobial Activities Evaluated in Brain-Heart Broth

	Compound	*E. coli* MIC	*E. coli* MBC	*P. aeruginosa* MIC	*P. aeruginosa* MBC	*S. aureus* MIC	*S. aureus* MBC
1	H-β-HLeu^u-β-HLys^u-β-HLeu^u-β-HLys^u-β-HPhe^u-β-HPhe^u-β-HLys^u-β-HLeu^u-β-HLys^u	>256	>256	>256	>256	>256	>256
2	H-β-HAla^u-β-HLys^u-β-HAla^u-β-HLys^u-β-HTyr^u-β-HTyr^u-β-HLys^u-β-HAla^u-β-Hlys^u	>256	>256	>256	>256	>256	>256
3	H-β-HTyr^u-β-HLys^u-β-HVal^u-β-HLys^u-β-HVal^u-β-HVal^u-β-HLys^u-β-HVal^u-β-HLys^u	>256	>256	>256	>256	>256	>256
4	H-β-HVal^u-β-HLys^u-β-HTrp^u-β-HVal^u-β-HLys^u-β-HVal^u-β-HLys^u-β-HVal^u-β-HLys^u	128	>256	>256	>256	>256	>256
5	H-β-HVal^u-β-HTrp^u-β-HLys^u-β-HTrp^u-β-HLys^u-β-HVal^u-β-HTrp^u-β-HLys^u	>256	>256	>256	>256	256	>256
6	H-β-HVal^u-β-HLys^u-β-HTrp^u-β-HVal^u-β-HLys^u-β-HTrp^u-β-HLys^u-β-HVal^u	32	128	128	>256	256	256
7	H-β-HVal^u-β-HLys^u-β-HTrp^u-β-HVal^u-β-HLys^u-β-HVal^u-β-HLys^u-β-HTrp^u	32–64	64–128	128	>256	64	>256
8	H-β-HVal^u-β-HLys^u-β-HPhe^u-β-HVal^u-β-HLys^u-β-HPhe^u-β-HLys^u-β-HVal^u	64–128	128	128	>256	64–128	>256
9	*i*Pr-NHCO-β-HVal^u-β-HTrp^u-β-HLys^u-β-HTrp^u-β-HLys^u-β-HVal^u-β-HTrp^u-β-HLys^u	128	>256	>256	>256	128	256
10	*i*Pr-NHCO-β-HVal^u-β-HLys^u-β-HTrp^u-β-HVal^u-β-HLys^u-β-HTrp^u-β-HLys^u-β-HVal^u	32	256	64	>256	32	32
11	Bz-NHCO-β-HVal^u-β-HLys^u-β-HTrp^u-β-HVal^u-β-HLys^u-β-HTrp^u-β-HLys^u-β-HVal^u	64	128	128	>256	32	64
12	*i*Pr-NHCO-β-HLys^u-β-HTrp^u-β-HVal^u-β-HLys^u-β-HTrp^u-β-HLys^u-β-HVal^u	>256	>256	>256	>256	128	>256
13	*i*Pr-NHCO-β-HVal^u-β-HLys^u-β-HTrp^u-β-HVal^u-β-HLys^u-β-HTrp^u-β-HLys^u	64–128	64–256	256	>256	32–64	64–128
14	Ac-Val-Lys-Trp-Val-Lys-Trp-Lys-Val	>256	>256	>256	>256	>256	>256
	Melittin	>256	>256	>256	>256	32	64

MIC and MBC in μg/ml.

(Table 1). In aqueous environment, the shape of the CD signal (one positive extremum at 203 nm) was conserved, but its intensity was reduced, indicating a significantly lower propensity for helix formation in aqueous environment (Figure 2F).

Shorter sequences (8-mers) with amphiphilic arrangement of β-HLys^u, β-HVal^u, and β-HTrp^u residues (**5–7**) were next evaluated. The rationale for choosing β-HVal^u residues came from the finding that **3** exhibits a particularly intense CD signature in MeOH (per residue molar ellipticity at 203 nm $\sim 7 \cdot 10^4$ deg · cm^2 · dmol^{-1}) characteristic of a stable *2.5*-helical structure (Figure 2A). Although valine is much less prone than alanine to α helix formation, it has been shown recently that β-amino acid residues bearing side chains branched at the first carbon (e.g., β^3-HVal) have a strong 3_{14} helix propensity [25, 26]. The CD spectrum of **3** may suggest the same trend for 2.5 helix formation with β-HVal^u residues. Although the

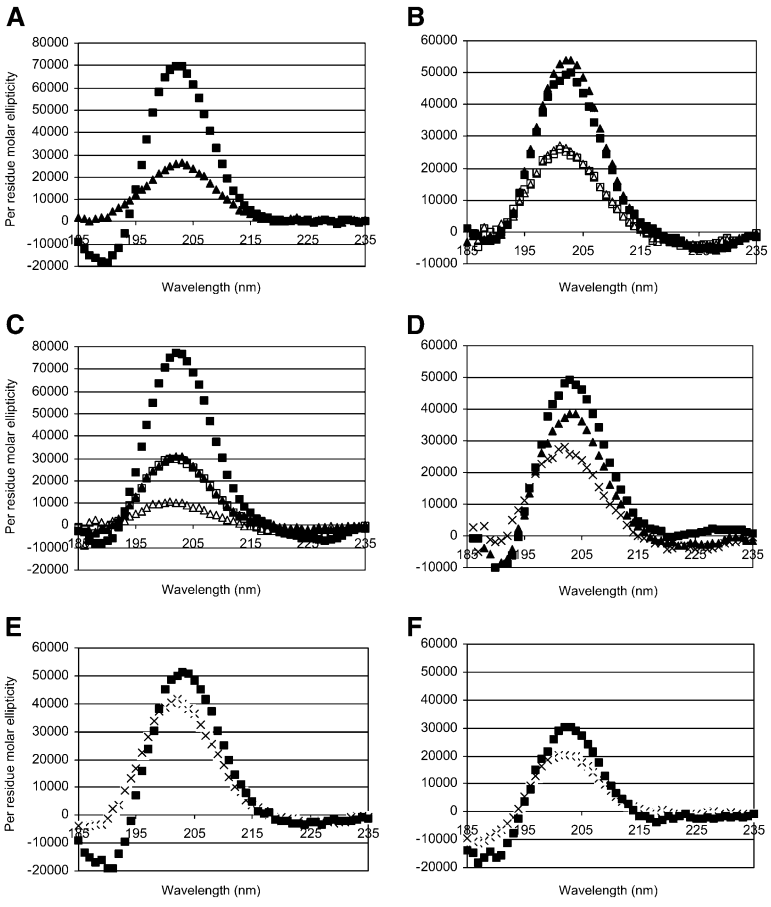

Figure 2. Helix-Forming Propensity of Oligoureas Investigated by Circular Dichroism in Various Media at 0.5 mM · per Residue Molar Ellipticity in deg · cm^2 · dmol^{-1}

(A) Closed square, molecule **3** in MeOH; closed triangle, molecule **2** in MeOH.

(B) Closed square molecule **12** in MeOH; closed triangle, molecule **13** in MeOH; open square, molecule **12** in HBS; open triangle molecule **13** in HBS (pH 7.4).

(C) Closed square, molecule **10** in MeOH; closed triangle, molecule **6** in MeOH, open square, molecule **10** in HBS (pH 7.4); open triangle, molecule **6** in HBS (pH 7.4).

(D) X, molecule **10** in HBS (pH 7.4); closed triangle, molecule **10** in zwitterionic liposomes (PC/Chol, 80:20, lipid/oligomer ratio of 5); closed square, molecule **10** in anionic liposomes (PC/PG 70:30, lipid/oligomer ratio of 10).

(E) X, molecule **11** in HBS (pH 7.4); closed square, molecule **11** in anionic liposomes (PC/PG 70:30, lipid/oligomer ratio of 10).

(F) X, molecule **3** in HBS (pH 7.4); closed square, molecule **3** in anionic liposomes (PC/PG 70:30, lipid/oligomer ratio of 10).

Table 2. Antimicrobial Activities Evaluated in Mueller-Hinton Broth

		E. coli		*P. aeruginosa*		*S. aureus*		MRSA	
	Compound	MIC	MBC	MIC	MBC	MIC	MBC	MIC	MBC
10	*i*Pr-NHCO-β-HVal^u-β-HLys^u-β-HTrp^u-β-HVal^u-β-HLys^u-β-HTrp^u-β-HLys^u-β-HVal^u	16	64	16	128	16	32	16	32
15	Cyclo((D)Arg-Arg-(D)Lys-Trp-(D)Leu-Trp-(D)Leu-Trp)	64	256	64	256	16	64	16	32
	Melittin	32	64	64	256	8	32	8	64

MIC and MBC in μg/ml. MRSA: methicillin resistant *Staphylococcus aureus*.

overall features of the *N,N′*-linked oligourea and β^3-peptide helices differ significantly, both helical backbones are characterized by synclinal arrangement around C(α)-C(β) bonds that may be stabilized when branched side chains are present [27]. The (1*H*-indol-3-yl)methyl side chain of β-HTrp^u was preferred over other aromatic hydrophobic side chains because of the known preference of tryptophan residues for membrane surfaces [28]. Tryptophan-rich sequence motifs are found in various natural (e.g., indolicidin [29] lactoferricin [30]) as well as in potent de novo designed [31, 32] antimicrobial peptides. Although compound **5** was inactive, octamers **6** and **7** displayed significant antibacterial activity against *E. coli* with a MIC of 32 μg/ml. Substitution of β-HPhe^u for β-HTrp^u residues in **6** to give **8**, decreased the activity against against *E. coli* and moderately improved activity against *S. aureus.*

We have shown previously that the helix stability can be significantly enhanced by acylating the free amino terminus of oligoureas [22]. This effect is believed to result from the removal of the repulsive charge-pole interaction between the protonated amino group and the positive pole of the helix, as well as from the presence of one additional H-bond acceptor. The effect of capping on antibacterial activity was thus considered. Oligomers **9** and **10** *N*-capped with isopropyl isocyanate were significantly more potent than their uncapped homologs **5** and **6**, respectively (Table 1). Particularly noteworthy is the pronounced inhibitory and bactericidal effect of compound **10** on *S. aureus* (MIC, 32 μg/ml; MBC, 32 μg/ml). Replacing the isopropyl urea terminus in **10** by a benzyl urea (**11**) only marginally affected the activity against *E. coli*. Two analogs of **10** shorter by one residue were synthesized by removing β-HVal^u at either terminus of the oligomer. Interestingly, while removal of the *N*-capped β-HVal^u residue (heptamer **12**) was detrimental for the activity, this modification when conducted at the opposite terminus to give heptamer **13**, had little effect on antimicrobial potency. Although **12** and **13** strongly differ in their antibacterial activity, they exhibit virtually identical CD spectra in MeOH and in HBS buffer (10 mM HEPES, 150 mM NaCl, 3 mM EDTA [pH 7.4]) at 0.5 mM (Figure 2D).

An α-peptide (**14**) containing Lys, Trp, and Val residues arranged in the same order as in **10** was synthesized and evaluated for comparison against the four bacterial strains. This peptide did not show any significant antibacterial activity (Table 1), thus suggesting that the unique structure of the urea backbone contributes to the observed antibacterial activity of oligoureas. This first screen revealed several trends. Antibacterial activities of oligoureas appear to depend on a fine balance between cationic, aliphatic, and aromatic side chains. The best results have been obtained when the number of amino groups (terminus and side chains) does not exceed 40% of the total number of side chains and when aromatic side chains represent no more than 50% of hydrophobic side chains. In addition, capping the free amino group of oligoureas appears to be a major determinant of antibacterial activity of *N,N′*-linked oligoureas.

After this initial screening process, additional experiments were conducted with **10**. When compound **10** was assayed by dilution method in Mueller-Hinton broth according to the National Committee for Clinical Laboratory Standards (NCCLS) guidelines, a significant gain in activity was observed on gram-negative bacteria, with MIC values of 16 μg/ml on *E. coli* and *P. aeruginosa.* Under these conditions, MIC and MBC values of 16 and 32 μg/ml, respectively were obtained on *S. aureus* ATCC 25923 and methicillin-resistant *S. aureus* (MRSA) (Table 2). Interestingly, in vitro activity of octamer **10** against MRSA was found to be equal to that of **15** (cyclo(D-Arg-Arg-D-Lys-Trp-D-Leu-Trp-D-Leu-Trp), an eight-residue cyclic D,L-α-peptide previously reported to be membrane active and to protect mice against MRSA lethal infection [33] (Table 2). The finding that **10** exhibits MICs and MBCs in the same value range and is equally potent on methicillin-sensitive and methicillin-resistant *S. aureus* strains is particularly noteworthy and suggests that **10** may be acting by a mechanism involving membrane permeation.

With the aim to correlate the antibacterial activity of **10** with its folding behavior, we have undertaken a series of CD experiments. As expected, **10** showed a high helical content in MeOH compared to uncapped **6** (3-fold increase in intensity at 203 nm) (Figure 2C). The value of the molar ellipticity per urea bond at 203 nm in MeOH (ca $8 \cdot 10^4$ deg $\cdot$ cm^2 $\cdot$ dmol^{-1}) is the highest observed so far for oligoureas (for comparison see [22]). Interestingly, the same trend was observed in HBS buffer at pH 7.4, with no particular change in the overall shape of the CD spectra (Figure 2C). However, the significantly weaker molar ellipticity values per urea bond at 203 nm in this solvent (ca 2.5-fold decrease for both **6** and **10**) were indicative of a lower propensity of oligoureas for helix formation in aqueous environment (Figure 2C). Changes in secondary structures that may occur upon binding to lipids can be investigated with liposomes as simplified model systems [34]. In the presence of negatively charged PC/PG (70:30) small unilamellar vesicles (SUV), the intensity of the maximum at 203 nm in the CD spectrum of **10** recorded between 185 and 250 nm experienced a sharp increase (ca $5 \cdot 10^4$ deg $\cdot$ cm^2 $\cdot$ dmol^{-1}) relative to aqueous solution, thus indicating that the *2.5*-helical conformation of **10** is stabilized in

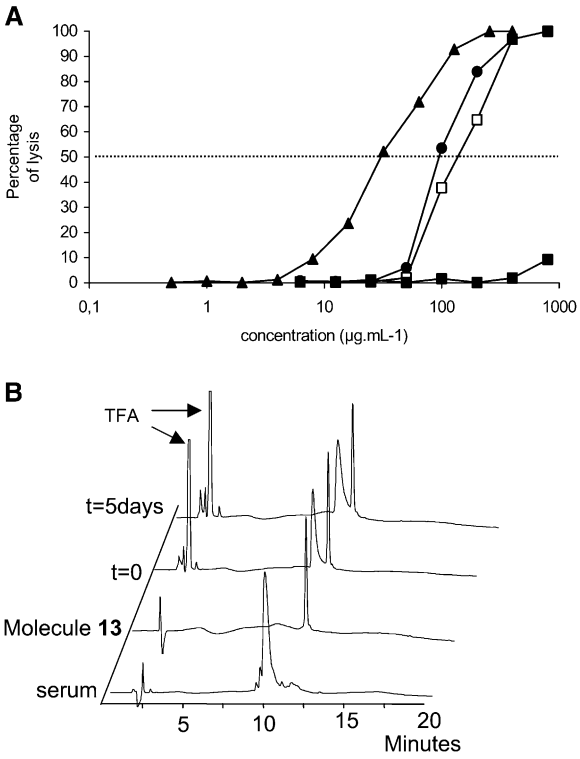

Figure 3. Hemolytic Activity and Stability of Oligoureas toward Proteolysis

(A) Hemolytic activity measured at indicated concentrations of Melittin (closed triangle), molecule **10** (open square), molecule **14** (closed square), and molecule **15** (closed circle).

(B) Proteolytic stability of molecule **13** evaluated by RP-HPLC after 5 days in mouse serum at 37ºC.

the presence of bacterial membrane-mimetic lipid vesicles (Figure 2D). A similar but attenuated behavior was observed in the presence of zwitterionic (PC/Chol) (80:20) lipid vesicles (Figure 2D). These data highlight the differential ability of anionic and zwitterionic liposomes to stabilize the *2.5*-helical structure and might suggest an increased specificity of **10** for anionic versus zwitterionic membranes. The same trend was observed for **11** (Figure 2E). In contrast, the intensity of the maximum at 203 nm measured in aqueous environment for inactive nonamer **3** (Figure 2F) in the presence of anionic lipid vesicles remained significantely lower. These results suggest that high *2.5*-helix propensity in lipidic environment may be a precondition for oligoureas to be active against bacteria.

Oligourea selectivity for prokaryotic cells was evaluated by monitoring lysis of human red blood cells. The hemolytic activity of molecule **10** compared to the corresponding α-peptide **14**, cyclo-D,L-α-peptide **15** and melittin is shown in Figure 3A. The concentration required for 50% red blood cell lysis (HC_{50}) together with selectivity values are reported in Table 3. While melittin is strongly toxic toward red blood cells (HC_{50} = 30 μg/ml in this assay), **10** exhibited significant selectivity for bacterial cells over human cells (selectivity value of 9.4 for both *E.coli* and *S. aureus*). The hemolytic activity of **10** in this assay was found to be slightly lower than that found for cyclic D,L-α-peptide **15**, which exhibits selectivity values of 3.1 and 6.3 for *E. coli* and *S. aureus*, respectively. The corresponding inactive α-peptide **14** did not show any hemolytic activity.

Table 3. Hemolytic Activity and Selectivity of Oligourea **10**

Compound	HC_{50}	Selectivity (HC_{50}/MIC)	
		E. coli	*S. aureus*
Melittin	30	1.9	3.75
10	150	9.4	9.4
15	100	3.1	6.3

HC_{50} in μg/ml. MIC (in μg/ml) were those obtained in Mueller-Hinton broth (see Table 2).

The susceptibility of oligoureas to proteolytic cleavage was assessed by incubating octamer **13** in mouse serum at 37ºC for different periods of time. After addition of TFA and centrifugation, the supernatant was analyzed by RP-HPLC. The area of the peak did not change significantly over a period of 5 days (Figure 3B), thus confirming the expected high resistance of oligoureas in serum.

Significance

In the field of biomimetic chemistry, several unnatural oligoamide backbones (peptoids, β-peptides, γ-peptides) have been described that self-organize at the molecular level to form stable helices useful to mimic protein secondary structure elements. The predictability of folding of these oligomeric strands led to the development of molecules with function including potent antibacterials [14–19] and inhibitors of protein-protein interactions [35–37]. Although the amide bond is undoubtedly a consensual motif for the elaboration of peptidomimetic folding oligomers ("foldamers"), we have shown that the urea moiety, by its capacity to form autocomplementary and bidirectional hydrogen bonds can be substituted for the amide linkage to generate oligomeric strands with strong propensity for helix formation [20–22]. The present work is the first attempt to design bioactive oligoureas based on their propensity to adopt *2.5*-helical structures. The finding that cationic amphiphilic oligoureas as short as 7–8 residues (e.g., 10) display significant antibacterial activity in vitro as well as membrane selectivity is promising. Like the α helix, the $2.5_{12,14}$ helix of enantiopure *N,N′*-linked oligoureas whose residues derive from natural L-α amino acids is right handed and polarized. Assuming an ideal *2.5*-helical structure and a pitch of 5.1 Å, octamer 10 is ca 16 Å long, which is equivalent in size to a 11 residue α-peptide in α-helical conformation. In comparison, the 26-residue melittin is ca 40 Å long when it is in an α-helical structure. Interestingly, while this paper was in preparation, Tew and coworkers [38] reported that substituting ureas for amides into antibacterial amphiphilic triarylamides [39] resulted in more potent and more selective compounds. This work further highlights the potential of the urea backbone for the development of antimicrobial agents. Studies aimed at improving the potency, the selectivity, as well as gaining further insight into the antibacterial mechanisms of *2.5*-helical oligoureas are underway in our laboratories.

Experimental Procedures

General

Amino-acid derivatives were purchased from NeoMPS (Strasbourg, France) and Rink amide resin from Senn Chemicals (Gentilly, France). All other reagents and solvents were of analytical grade. Analytical HPLC was performed by using a Varian apparatus on a Nucleosil C_{18} (150 mm × 4.6 mm, 5 μ particle column) by using a linear gradient of A (0.1% TFA in H_2O) and B (0.08% TFA in CH_3CN) at a flow rate of 1.2 ml/min. Preparative reverse-phase HPLC were performed by using a Beckman apparatus on a Nucleodur C_{18} (250 mm × 10 mm, 16 μ particle column) by elution with a linear gradient of A (0.1% TFA in H_2O) and B (0.08% TFA in CH_3CN), at a flow rate of 6 ml/min with UV detection at 210 nm. Mass spectra were obtained by matrix-assisted laser desorption/ionization mass spectrometry (MALDI-MS) on a Protein TOF apparatus (Bruker Spectrospin, Bremen, Germany).

Oligoureas Synthesis and Purification

Oligoureas were prepared by Fmoc chemistry on a home made multichannel synthesizer with a semiautomatic mode on a 30–40 μmol scale starting from Rink amide Resin (0.8 mmol/g). The Fmoc group was removed with 25% piperidine in DMF (20 min) under nitrogen bubbling. The resin was then filtered and washed with DMF (5 × 1 min). For each coupling step, a solution of succinimidyl carbamate (five equiv.) in DMF was added on the resin, and the suspension was mixed under periodic nitrogen bubbling for 120 min. Completion of the coupling of the first carbamate building block was monitored by a Kaiser ninhydrin test, and the remaining coupling steps were performed in blind. A double coupling was performed systematically. At the end of the synthesis, the resin was washed with CH_2Cl_2, Et_2O, and dried under nitrogen. Sidechain deprotection and cleavage of the oligomers from the resin were performed simultaneously by treatment with TFA/H_2O/triisopropylsilane (95:2.5:2.5) for 150 min at 20ºC. The TFA solution were concentrated in vacuo, solubilized in H_2O/MeCN (9:1) and lyophilized to afford crude oligomers. The crude oligomers were finally purified by RP-HPLC (linear gradient, 5%–65% or 20%–80% B, 30 min) to a final purity ≥95% and lyophilized.

Oligomer 1

Purity of crude product 16% (C_{18} RP-HPLC). Yield after purification: 3 mg, 5%; white powder; RP-HPLC t_R 15.6 min (linear gradient, 5%–65% B, 20 min); MS (MALDI-TOF) m/z 1426.2 $[M + H]^+$, 1446.5 $[M + Na]^+$, 1463.3 $[M + K]^+$.

Oligomer 2

Purity of crude product 32% (C_{18} RP-HPLC). Yield after purification: 6 mg, 10%; white powder; RP-HPLC t_R 9.8 min (linear gradient, 5%–65% B, 20 min); MS (MALDI-TOF) m/z 1330.0 $[M + H]^+$.

Oligomer 3

Purity of crude product 18% (C_{18} RP-HPLC). Yield after purification: 3 mg, 5%; white powder; RP-HPLC t_R 12.1 min (linear gradient, 5%–65% B, 20 min); MS (MALDI-TOF) m/z 1350.5 $[M + H]^+$.

Oligomer 4

Purity of crude product 18% (C_{18} RP-HPLC). Yield after purification: 3 mg, 5%; white powder; RP-HPLC t_R 13.9 min (linear gradient, 5%–65% B, 20 min); MS (MALDI-TOF) m/z 1051.5 $[M + H]^+$, 1073.3 $[M + Na]^+$.

Oligomer 5

Purity of crude product 33% (C_{18} RP-HPLC). Yield after purification: 4 mg, 7%; white powder; RP-HPLC t_R 13.7 min (linear gradient, 5%–65% B, 20 min); MS (MALDI-TOF) m/z 1414.0 $[M + Na]^+$, 1445.0 $[M + K]^+$.

Oligomer 6

Purity of crude product 23% (C_{18} RP-HPLC). Yield after purification: 4 mg, 10%; white powder; RP-HPLC t_R 14.4 min (linear gradient, 5%–65% B, 20 min); MS (MALDI-TOF) m/z 1326.0 $[M + Na]^+$, 1357.0 $[M + K]^+$.

Oligomer 7

Purity of crude product 15% (C_{18} RP-HPLC). Yield after purification: 6mg, 9%; white powder; RP-HPLC t_R 13.60 min (linear gradient, 5%–65% B, 20 min); MS (MALDI-TOF) m/z 1305.1 $[M + H]^+$, 1329.1 $[M + K]^+$.

Oligomer 8

Purity of crude product 24% (C_{18} RP-HPLC). Yield after purification: 10mg, 15%; white powder; RP-HPLC t_R 13.3 min (linear gradient, 5%–65% B, 20 min); MS (MALDI-TOF) m/z 1247.9 $[M + Na]^+$.

Oligomer 9

Purity of crude product 18% (C_{18} RP-HPLC). Yield after purification: 3 mg, 7%; white powder; RP-HPLC t_R 17.4 min (linear gradient, 5%–65% B, 20 min); MS (MALDI-TOF) m/z 1475.1 $[M + H]^+$, 1496.5 $[M + Na]^+$.

Oligomer 10

Purity of crude product 17% (C_{18} RP-HPLC). Yield after purification: 4 mg, 6%; white powder; RP-HPLC t_R 11.4 min (linear gradient, 20%–80% B, 20 min); MS (MALDI-TOF) m/z 1390.6 $[M + H]^+$, 1414.4 $[M + Na]^+$.

Oligomer 11

Purity of crude product 18% (C_{18} RP-HPLC). Yield after purification: 6 mg, 8%; white powder; RP-HPLC t_R 11.6 min (linear gradient, 20%–80% B, 20 min); MS (MALDI-TOF) m/z 1459.0 $[M + Na]^+$.

Oligomer 12

Purity of crude product 18% (C_{18} RP-HPLC). Yield after purification: 10 mg, 16%; white powder; RP-HPLC t_R 10.2 min (linear gradient, 20%–80% B, 20 min); MS (MALDI-TOF) m/z 1282.8 $[M + Na]^+$.

Oligomer 13

Purity of crude product 21% (C_{18} RP-HPLC). Yield after purification: 7 mg, 11%; white powder; RP-HPLC t_R 11.1 min (linear gradient, 20%–80% B, 20 min); MS (MALDI-TOF) m/z 1260.8 $[M + H]^+$, 1282.8 $[M + Na]^+$.

Preparation of Liposomes

The phospholipids egg yolk L-α-phosphatidylcholine (PC) and L-α-phosphatidyl-DL-glycerol (PG) transesterified from egg yolk PC were purchased from Sigma-Aldrich (Saint-Quentin-Fallavier, France). Liposomes were prepared by mixing, in a round-bottom flask, phospholipids (PC, PG) and cholesterol (PC/PG 70:30 and PC/Cholesterol 80:20) in chloroform/methanol 9:1. After solvent evaporation under high vacuum, the dried lipid film was hydrated by Vortex mixing after addition of 1 ml HBS buffer (for 10 μmol lipids) (10 mM HEPES, 150 mM NaCl, 3 mM EDTA [pH 7.4]). The resulting suspensions were sonicated at 25ºC for 1 hr (5 s cycles interrupted for 1.25 s) under a continuous flow of argon, with a 3 mm diameter probe sonicator (Vibra Cell, Sonics and Material, Inc., Danbury, CT) at 300 W. The SUV preparations were finally centrifuged for 10 min at 10,000 × g to remove both the titanium dust originating from the probe and the lipid aggregates. The size of the liposomes was determined by dynamic light scattering with a Zeta-master 3000 instrument (Malvern Instruments, Paris, France). Data were collected with the multimodal number distribution software included in the instrument. All the formed vesicles were uniformly distributed in size and exhibited average diameters of 100 nm (±20 nm). The final lipid concentration of the liposomal suspensions was determined by enzymatic titration of phosphatidyl choline (phospholipid B test WACO COF was purchased from OXOID [Dardilly, France]). All the liposomal formulations were freshly prepared before use.

Circular Dichroism

All circular dichroism (CD) spectra were recorded on a J-810 Jasco spectropolarimeter 150S (Jasco France, Nantes, France). Data are expressed in term of mean-residue ellipticity in $deg \cdot cm^2 \cdot dmol^{-1}$, calculated per mol of urea groups present. CD spectra of oligomers (0.5 mM) were aquired in MeOH and in HBS buffer (10 mM HEPES, 150 mMNaCl, 3 mM EDTA [pH 7.4]) at 25ºC, between 190 and 250 nm by using a quartz cylindrical cell with a path length of 0.05 mm (Hellma 121-QS-0.05, Paris, France). Experiments in presence of liposomes were conducted with a ratio lipid/oligomer of five for zwitterionic formulation (PC/Cholesterol 80:20) and ten for anionic formulation (PC/PG 70:30), the concentration of oligomer remaining 0.5 mM. Minor contributions of circular differential scattering by liposomes were eliminated by substraction of the CD spectrum of liposomes alone.

In Vitro Susceptibility of Aerobic Bacteria

Four strains were selected: *Escherichia coli* ATCC 25922, *Staphylococcus aureus* ATCC 25923, *Pseudomonas aeruginosa* ATCC 27853, and a clinical isolated methicillin resistant *Staphylococcus aureus* strain. Antibacterial activity of the molecules was tested by dilution method in Brain-Heart broth (BioRad, Marnes-la-Coquette) or in Mueller-Hinton broth (Difco, Becton-Dickinson France, Le Pont de Claix) in order to determine the minimal inhibitory

concentration (MIC) and the minimal bactericidal concentration (MBC). Stock solutions were obtained by solubilizing molecule powders in sterile distillated water at concentration of 2.56 mg/ml and serial 2-fold diluted solutions were prepared. Bacterial inoculum was standardized by using direct suspensions of colonies from overnight growth in saline adjusted to a turbidity matching that of a 0.5 McFarland standard, (10^8 CFU/ml) and diluted to obtain a density comprised between 10^5 CFU/ml and 10^7 CFU/ml. Tubes containing 900 μl of inoculum with 100 μl of molecules solutions were incubated in air at 35ºC for 18 to 20 hr before the MICs were determined. Purity and inoculum density as well as percentage of viable bacteria in limpid tubes were checked by plate counting on sheep blood agar. Broth without any molecule solution was inoculated with each selected bacterial strain as a control for organism viability (growth control). The susceptibility of *S. aureus* strains against a glycopeptide (vancomycin) was used as an internal control as well as the activity of melittin.

In Vitro Hemolysis Assay

Human blood collected on heparin was centrifuged at 1,000 × g for 10 min to remove serum. Red blood cells were then washed three times with 0.9% saline solution and resuspended to a concentration of 5% in saline solution containing 10% FBS (v/v). Red blood cells were then incubated with serial dilution of the molecules at 37ºC for 1 hr. Control samples included a saline solution as negative control and 1% Triton X-100 for 100% hemolysis. For measurement of hemoglobin content, plates were centrifuged at 1,000 × g for 5 min, and aliquots of the supernatant were read at 570 nm.

Proteolytic Degradation

Oligomer 10 (1 μg/ml in PBS) was incubated at 37ºC with the same volume of BALB/c serum freshly collected. For analysis, 50 μl of solution was collected, and 5 μl of TFA was added to precipitate serum proteins. After addition of 200 μl of PBS buffer, solutions were centrifugated for 15 min. Supernatants were diluted twice and analyzed by RP-HPLC. (C18 column, linear gradient, 20%–80% B, 20 min.)

Acknowledgments

This research was supported in part by Centre National de la Recherche Scientifique (CNRS, soutien jeune équipe), Région Alsace, and ImmuPharma France. Fellowships from ImmuPharma France and Région Alsace for A.V. and K.L. are gratefully acknowledged.

Received: October 14, 2005
Revised: March 20, 2006
Accepted: March 24, 2006
Published: May 29, 2006

References

1. Habermann, E. (1972). Bee and wasp venoms. Science *177*, 314–322.
2. Zasloff, M. (1987). Magainins, a class of antimicrobial peptides from *Xenopus* skin: isolation, characterization of two active forms, and partial cDNA sequence of a precursor. Proc. Natl. Acad. Sci. USA *84*, 5449–5453.
3. Steiner, H., Hultmark, D., Engstrom, A., Bennich, H., and Boman, H.G. (1981). Sequence and specificity of two antibacterial proteins involved in insect immunity. Nature *292*, 246–248.
4. Zasloff, M. (2002). Antimicrobial peptides of multicellular organisms. Nature *415*, 389–395.
5. Ge, Y., MacDonald, D.L., Holroyd, K.J., Thornsberry, C., Wexler, H., and Zasloff, M. (1999). In vitro antibacterial properties of pexiganan, an analog of magainin. Antimicrob. Agents Chemother. *43*, 782–788.
6. Dartois, V., Sanchez-Quesada, J., Cabezas, E., Chi, E., Dubbelde, C., Dunn, C., Granja, J., Gritzen, C., Weinberger, D., Ghadiri, M.R., et al. (2005). Systemic antibacterial activity of novel synthetic cyclic peptides. Systemic antibacterial activity of novel synthetic cyclic peptides. Antimicrob. Agents Chemother. *49*, 3302–3310.
7. Hancock, R.E., and Chapple, D.S. (1999). Peptide antibiotics. Antimicrob. Agents Chemother. *43*, 1317–1323.
8. Shai, Y. (2002). Mode of action of membrane active antimicrobial peptides. Biopolymers *66*, 236–248.
9. McDonald, D.L., Beyermann, M., and Bienert, M. (1997). Hydrophobicity, hydrophobic moment and angle subtended by charged residues modulate antibacterial activity of amphipathic helical peptides. FEBS Lett. *403*, 208–212.
10. Dathe, M., and Wieprecht, T. (1999). Structural features of helical antimicrobial peptides: their potential to modulate activity on model membranes and biological cells. Biochim. Biophys. Acta *1462*, 71–87.
11. Guichard, G. (2004). β-Peptides, γ-peptides and isosteric backbones: new scaffolds with controlled shapes for mimicking protein secondary structure elements. In Pseudopeptides in Drug Development, P.E. Nielsen, ed. (Weinheim, Germany: Wiley-VCH Verlag), pp. 33–120.
12. Seebach, D., Beck, A.K., and Bierbaum, D.J. (2004). The world of β- and γ-peptides comprised of homologated proteinogenic amino acids and other components. Chem. Biodiv. *1*, 1111–1239.
13. Cheng, R.P., Gellman, S.H., and DeGrado, W.F. (2001). β-Peptides: from structure to function. Chem. Rev. *101*, 3219–3232.
14. Porter, E.A., Wang, X., Lee, H.S., Weisblum, B., and Gellman, S.H. (2000). Non-haemolytic beta-amino-acid oligomers. Nature *404*, 565. Erratum: Nature *405*(6784), 298.
15. Porter, E.A., Weisblum, B., and Gellman, S.H. (2002). Mimicry of host-defense peptides by unnatural oligomers: antimicrobial beta-peptides. J. Am. Chem. Soc. *124*, 7324–7330.
16. Raguse, T.L., Porter, E.A., Weisblum, B., and Gellman, S.H. (2002). Structure-activity studies of 14-helical antimicrobial beta-peptides: probing the relationship between conformational stability and antimicrobial potency. J. Am. Chem. Soc. *124*, 12774–12785.
17. Liu, D., and DeGrado, W.F. (2001). De novo design, synthesis, and characterization of antimicrobial β-peptides. J. Am. Chem. Soc. *123*, 7553–7559.
18. Arvidsson, P.I., Ryder, N.S., Weiss, H.M., Gross, G., Kretz, O., Woessner, R., and Seebach, D. (2003). Antibiotic and hemolytic activity of a β2/β3 peptide capable of folding into a 12/10-helical secondary structure. ChemBioChem *4*, 1345–1347.
19. Patch, J.A., and Barron, A.E. (2003). Helical peptoid mimics of magainin-2 amide. J. Am. Chem. Soc. *125*, 12092–12093.
20. Semetey, V., Rognan, D., Hemmerlin, C., Graff, R., Briand, J.-P., Marraud, M., and Guichard, G. (2002). Stable helical secondary structure in short chain N,N′-linked oligoureas bearing proteinogenic side chains. Angew. Chem. Int. Ed. Engl. *41*, 1893–1895.
21. Hemmerlin, C., Marraud, M., Rognan, D., Graff, R., Semetey, V., Briand, J.-P., and Guichard, G. (2002). Helix forming oligoureas: temperature-dependent NMR, structure determination and circular dichroism of a nonomer with functionalised side chain. Helv. Chim. Acta *85*, 3692–3711.
22. Violette, A., Averlant-Petit, M.C., Semetey, V., Hemmerlin, C., Casimir, R., Graff, R., Marraud, M., Briand, J.-P., Rognan, D., and Guichard, G. (2005). N,N′-linked oligoureas as foldamers: chain length requirements for helix formation in protic solvent investigated by circular dichroism, NMR spectroscopy and molecular dynamics. J. Am. Chem. Soc. *127*, 2156–2164.
23. Guichard, G., Semetey, V., Rodriguez, M., and Briand, J.-P. (2000). Solid phase synthesis of oligoureas using O-succinimidyl-(9H-fluoren-9-ylmethoxycarbonylamino)-ethyl carbamate derivatives. Tetrahedron Lett. *41*, 1553–1557.
24. Guichard, G., Semetey, V., Didierjean, C., Aubry, A., Briand, J.-P., and Rodriguez, M. (1999). An effective preparation of O-succinimidyl-2-(tert-butoxycarbonylamino)-ethylcarbamate derivatives from β-amino-acids. Application to the synthesis of urea-containing pseudopeptides and oligoureas. J. Org. Chem. *64*, 8702–8705.
25. Raguse, T.L., Lai, J.R., and Gellman, S.H. (2002). Evidence that the β-peptide 14-helix is stabilized by β^3-residues with side-chain branching adjacent to the β-carbon atom. Helv. Chim. Acta *85*, 4154–4164.
26. Kritzer, J.A., Tirado-Rives, J., Hart, S.A., Lear, J.D., Jorgensen, W.L., and Schepartz, A. (2005). Relationship between side chain structure and 14-helix stability of β^3-peptides in water. J. Am. Chem. Soc. *127*, 167–178.

27. Martinek, T.A., and Fülöp, F. (2003). Side-chain control of β-peptide secondary structures. Eur. J. Biochem. (Tokyo) *270*, 3657–3666.
28. Yau, W.-M., Wimley, W.C., Gawrisch, K., and White, S.H. (1998). The preference of tryptophan for membrane interfaces. Biochemistry *37*, 14713–14718.
29. Selsted, M.E., Novotny, M.J., Morris, W.L., Tang, Y.Q., Smith, W., and Cullor, J.S. (1992). Indolicidin, a novel bactericidal tridecapeptide amide from neutrophils. J. Biol. Chem. *267*, 4292–4295.
30. Vogel, H.J., Schibli, D.J., Jing, W., Lohmeier-Vogel, E.M., Epand, R.F., and Epand, R.M. (2002). Towards a structure—function analysis of bovine lactoferricin and related tryptophan- and arginine-containing peptides. Biochem. Cell Biol. *80*, 49–63.
31. Deslouches, B., Phadke, S.M., Lazarevic, V., Cascio, M., Islam, K., Montelaro, R.C., and Mietzner, T.A. (2005). De novo generation of cationic antimicrobial peptides: influence of length and tryptophan substitution on antimicrobial activity. Antimicrob. Agents Chemother. *49*, 316–322.
32. Blondelle, S.E., and Lohner, K. (2000). Combinatorial libraries: a tool to design antimicrobial and antifungal peptide analogues having lytic specificities for structure—activity relationship studies. Biopolymers *55*, 74–87.
33. Fernandez-Lopez, S., Kim, H.S., Choi, E.C., Delgado, M., Granja, J.R., Khasanov, A., Kraehenbuehl, K., Long, G., Weinberger, D.A., Wilcoxen, K.M., et al. (2001). Antibacterial agents based on the cyclic D,L-alpha-peptide architecture. Nature *412*, 452–455.
34. Epand, R.M., and Epand, R.F. (2003). Liposomes as models for antimicrobial peptides. Methods Enzymol. *372*, 124–133.
35. Stephens, O.M., Kim, S., Welch, B.D., Hodsdon, M.E., Kay, M.S., and Schepartz, A. (2005). Inhibiting HIV fusion with a β-peptide foldamer. J. Am. Chem. Soc. *127*, 13126–13127.
36. Kritzer, J.A., Stephens, O.M., Guarracino, D.A., Reznik, S.K., and Schepartz, A. (2005). β-Peptides as inhibitors of protein-protein interactions. Bioorg. Med. Chem. *13*, 11–16.
37. Kritzer, J.A., Lear, J.D., Hodsdon, M.E., and Schepartz, A. (2004). Helical β-peptide inhibitors of the p53-hDM2 interaction. J. Am. Chem. Soc. *126*, 9468–9469.
38. Tang, H., Doerksen, R.J., and Tew, G.N. (2005). Synthesis of urea oligomers and their antibacterial activity. Chem. Commun. 1537–1539.
39. Tew, G.N., Liu, D., Chen, B., Doerksen, R.J., Kaplan, J., Carroll, P.J., Klein, M.L., and DeGrado, W.F. (2002). De novo design of biomimetic antimicrobial polymers. Proc. Natl. Acad. Sci. USA *99*, 5110–5114.